Biophysical Journal Volume 72 February 1997 754–766

Involvement of the Calcium Inward Current in Cardiac Impulse Propagation: Induction of Unidirectional Conduction Block by Nifedipine and Reversal by Bay K 8644

Stephan Rohr and Jan P. Kucera
Department of Physiology, University of Bern, CH-3012 Bern, Switzerland

ABSTRACT In general, the fast sodium inward current (I_{Na}) is regarded as the main inward current ensuring fast and safe excitation of the normally polarized working myocardium. However, under conditions of locally delayed excitation in the millisecond range, the slow inward current (I_{Ca}) might additionally contribute to the success of impulse propagation. This hypothesis was tested in patterned growth cultures of neonatal rat ventricular myocytes, which consisted of narrow cell strands connected to large rectangular cell monolayers, where I_{Na} or I_{Ca} could be modified in the narrow cell strand adjacent to the expansion by a microsuperfusion system. As assessed during antegrade (strand → expansion) propagation under control conditions using a system for multiple site optical recording of transmembrane voltage (MSORTV), this cell pattern gave either rise to local activation delays at the expansion ranging from 0.5 to 4 ms ($d_{control}$), or it induced undirectional conduction blocks (UCBs) in the antegrade direction. Irrespective of the size of $d_{control}$, suppression of the sodium current with tetrodotoxin confined to the cell strand adjacent to the expansion invariably induced UCB in the antegrade direction. If $d_{control}$ was >1 ms, UCB could also be elicited by suppression of I_{Ca} alone with nifedipine. Conversely, if UCB was present under control conditions, the inclusion of Bay K 8644 in the microsuperfusion established successful bidirectional conduction. These results suggest that I_{Ca} can be critically important for the success of impulse propagation across abrupt expansions of excitable tissue even if I_{Na} is not concurrently depressed.

INTRODUCTION

Impulse propagation in the heart is determined by both active and passive properties of the cardiac tissue, where active properties include ion channels, ion exchangers, and ion pumps, whereas passive properties refer to membrane resistance and capacitance, size and shape of individual myocytes, three-dimensional cell assemblage, topology and density of gap junctions, and the spatial organization of the extracellular space. In the past, fast and safe impulse conduction under physiological conditions in the working myocardium and in the His-Purkinje system was associated with the fast sodium inward current (I_{Na}), while conduction in the AV node was attributed to the slow calcium inward current (I_{Ca}) (Fozzard, 1990). This clear separation of ionic currents responsible for propagation in defined regions of the heart is, to some extent, lost under pathophysiological conditions. Thus, slow conduction occurring in partially depolarized myocardium can change from being mostly dependent on residual I_{Na} to being dependent on I_{Ca} in the presence of catecholamines (Hisatome and Arita, 1995). Under conditions of normal resting potentials, evidence has recently been presented that I_{Ca} can be critical for the success of action potential conduction from one ventricular myocyte to another (Sugiura and Joyner, 1992). These studies showed that if two individually patched single myocytes are coupled by means of a relatively high extrinsic resistor, impulse propagation fails during application of calcium channel blockers to the leader cell. This finding was explained by the nifedipine-induced reduction of inward current flowing during the plateau, which, in the presence of a large activation delay between the two cells, develops into a critical current source for the activation of the follower cell. While both of these conditions (partial depolarization and uncoupling) leading to I_{Ca}-dependent propagation, may be linked to pathophysiological settings (e.g., hypoxia and ischemia), it can be hypothesized that, in general, any situation causing a localized conduction delay of sufficient magnitude might render I_{Ca} important for the success of impulse propagation in the continued presence of I_{Na}.

Along this line of reasoning, it is well known that abrupt geometrical expansions of excitable tissue induce localized activation delays during conduction from small to large tissue areas. In this situation, which is present at the Purkinje fiber ventricular junction (Mendez et al., 1970; Veenstra et al., 1984), at the transition from the small SA node to the large atrium (Joyner and Van Capelle, 1986) or in surviving tissue islands in infarct scars (Ursell et al., 1985; de Bakker et al., 1993), the excitatory inward current delivered by a small cell mass in front of a given expansion might only be marginally sufficient to excite the larger tissue mass beyond the expansion (current-to-load mismatch) and, as a consequence, the slow charging of the membrane capacitance of the cells beyond the site of expansion gives rise to a localized conduction delay. The characteristics of the conduction process across geometrical expansions of ventricular tissue at the microscopic scale were recently investigated using patterned growth heart cell

Received for publication 11 July 1996 and in final form 2 October 1996.

Address reprint requests to Stephan Rohr, M.D., Dept. of Physiology, University of Bern, Bühlplatz 5, CH-3012 Bern, Switzerland. Tel.: 41-31-631-87-02; Fax: 41-31-631-46-11; E-mail: rohr@pyl.unibe.ch.

Part of this work has appeared in abstract form (Rohr and Kucera, 1995).

0006-3495/97/02/754/13 $2.00

cultures in conjunction with multiple-site optical recording of transmembrane voltage (MSORTV). In this model system consisting of a homogeneous cell population forming a geometrically defined tissue expansion, it was shown that the size of the propagation delay occurring at the site of the expansion is a function of the diameter of the cell strand in front of the expansion (Fast and Kléber, 1995a; Fast and Kléber, 1995b) and, furthermore, is dependent on the geometry of the expansion itself (Rohr and Salzberg, 1994a). Because these cultured cells express, besides sodium channels (Robinson, 1982; Rohr et al., 1991), also L-type calcium channels at a density similar to in-vivo adult myocardial tissue of the same species (Gomez et al., 1994), we thought them ideally suited to test the question whether I_{Ca} at the site of a current-to-load mismatch might be essential for the success of propagation in the continued presence of the sodium current. To this purpose, we constructed narrow cell strands connected to large rectangular tissue areas and altered pharmacologically the size of I_{Ca} of the current source by superfusing the narrow cell strand in front of the expansion with nifedipine or Bay K 8644. With these interventions, we could show that, in the setting of moderate current-to-load mismatches generating delayed but successful antegrade propagation, a reduction of I_{Ca} favors the formation of unidirectional conduction blocks (UCB). Conversely, in preparations exhibiting large current-to-load mismatches causing UCB under control conditions, an increase of I_{Ca} establishes bidirectional conduction.

MATERIALS AND METHODS

Patterned growth cell cultures

Cell cultures were prepared according to previously published procedures (Rohr et al., 1991). In short, hearts from 8 to 10 neonatal rats (Wistar, 1–2 days old) were excised, the ventricles were minced with scissors, and the resulting small tissue pieces were dissociated in Hanks' balanced salt solution (without Ca^{2+} and Mg^{2+}; Gibco, Basel, Switzerland) containing trypsin (0.1%, Boehringer, Rotkreuz, Switzerland) and pancreatin (60 μg/ml, Sigma, Buchs, Switzerland). The dispersed cells were, after centrifugation, resuspended in medium M199 (Gibco, Basel, Switzerland) with an ionic composition of (in mM): NaCl 137, KCl 5.4, $CaCl_2$ 1.3, $MgSO_4$ 0.8, $NaHCO_3$ 4.2, KH_2PO_4 0.5, NaH_2PO_4 0.3. The medium was supplemented with penicillin (20 U/ml; Fakola, Basel, Switzerland), streptomycin (20 μg/ml; Fakola, Basel, Switzerland), vitamin B_{12} (20 μg/ml; Sigma, Buchs, Switzerland), 100 μM bromodeoxyuridine (Sigma, Buchs, Switzerland) and 10% neonatal calf serum (Boehringer, Rotkreuz, Switzerland). The cell suspension was preplated in large culture flasks to reduce the fibroblast content, and the myocytes remaining in suspension were seeded at a density of 5×10^5 cells/ml (1.9×10^3 cells/mm^2) on conditioned coverslips. The cultures were kept in an incubator at 35°C in a humidified atmosphere containing 1.2% CO_2. Medium exchanges were performed on the first day after seeding and every other day thereafter with supplemented medium M199 containing a reduced concentration of serum (5%) and, at the occasion of the first medium exchange only, 10 μM epinephrine and 100 μM bromodeoxyuridine (both from Sigma, Buchs, Switzerland).

Experiments were performed with monolayer cultures having a defined two-dimensional geometry. The geometrical patterns were obtained using previously described photolithographic techniques (Rohr et al., 1991). In short, coverslips (22-mm diameter, 0.14-mm thickness, Haska, Switzerland) were coated with a photoresist (KTFR; Kodak, Lausanne, Switzerland), which prevented the adhesion of myocytes. The two-dimensional growth designs were etched into the photoresist and the resulting photoresist-free regions were coated with collagen Type IV (human placenta, Sigma, Buchs, Switzerland), which was dissolved at a concentration of 20 μg/ml in HBSS containing 12% (v/v) glacial acid. After seeding, cells preferentially attached to the photoresist-free regions of the coverslips, thereby forming the desired patterns. The patterns consisted either of linear cell strands (10 mm long, 50–70 μm wide) or of linear strands (1.8 mm long, 30–80 μm wide) connected to large rectangular cell areas (2.2 × 2.2 mm). In both types of patterns, the strands were connected to a ring-shaped monolayer of myocytes in the periphery of the round coverslips, which served to condition the medium and served as a pacemaker for the patterned growth cells ("feeder ring"). Both effects of the feeder ring, i.e., conditioning and pacemaking, increased the degree of phenotypic differentiation of the patterned growth cells (Rohr et al., 1991).

Experimental protocol

Experiments were performed with cultures 5–10 days old. The connections to the "feeder ring" were severed and the preparations were mounted in a temperature-controlled experimental chamber (Rohr, 1986), which was transferred to the stage of an inverted microscope (Axiovert 135 M, Zeiss, Switzerland). The thin coverslips formed the bottom of the chamber, thus permitting the use of short-working-distance objectives with high-numerical apertures. The preparations were aligned horizontally to the center of the field of view of the microscope and, in the case of the abrupt expansions, the site of expansion was centered as well. Immediately after mounting, superfusion with the control bath solution was started [HBSS, containing (in mM) NaCl 137, KCl 5.4, $CaCl_2$ 1.3, $MgSO_4$ 0.8, $NaHCO_3$ 4.2, KH_2PO_4 0.5, NaH_2PO_4 0.3, and Hepes 10, which was titrated to pH 7.40 with NaOH]. After constant temperatures were reached (36 ± 0.4°C), the preparations were stained for 3–4 min with 1 ml HBSS containing 135 μM of the voltage sensitive dye di-8-ANEPPS (Molecular Probes, Eugene, OR). The staining solution was freshly prepared from a stock solution of the dye containing 13.5 mM di-8-ANEPPS in DMSO/F127 (75%:25%, w/w; Fluka, Buchs, Switzerland, and BASF, Ludwigshafen, Germany). The preparations were stimulated with bipolar electrodes consisting of glass micropipettes filled with HBSS containing 1% agar and a silver wire coiled around the shank of the electrode, which were attached to micromanipulators (DC-3K, Märzhäuser, Wetzlar, Germany). The electrodes were placed at sufficient distance from the site of measurement to exclude stimulation artifacts and to permit propagation to reach steady-state conditions. Rectangular impulses (duration: 1 ms, twice threshold intensity) were delivered to the preparations at a basic cycle length of 500 ms by a stimulator (SD9, Grass Instrument Co., Quincy, MA) for at least 10 s before a given optical recording. The preparations were routinely stimulated from either side of the recording area to assure, before any interventions, that impulse conduction was symmetrical and continuous in the case of linear cell strands and to assess the degree of asymmetry in the case of abrupt tissue expansions. Conduction from the thin cell strand to the expansion was termed "antegrade," while the reverse direction of propagation was denoted as "retrograde." Usually, impulse propagation characteristics were recorded under control conditions, during a given intervention and during washout, resulting, due to the bidirectional stimulation protocol, in a total of six optical measurements per given location.

Local superfusion

To deliver drugs to the preparations in a spatially controlled manner, a local superfusion system was installed (Streit and Lux, 1989). In brief, the drug containing superfusate was delivered to the surface of the preparation by means of an extruded polyethylene tube (inner diameter of mouth = 200 μm), which was placed close to the target location and which was connected to a syringe pump (B.Braun Typ 1830, Melsungen, Germany). Removal of the superfusate by means of a second extruded tube connected to a vacuum pump (N 022, Ismatec, Zürich, Switzerland) was achieved by letting this tube face the inlet tube. Both tubes were attached to a micro-

manipulator (DC-3K, Märzhäuser, Wetzlar, Germany) permitting an exact positioning of the superfusion. By keeping the pump rate constant at 100 μl/min and changing the distance between inlet and outlet tube, the width of the stream of the superfusion solution could be varied between 200 μm and 1000 μm. The sizing and positioning of the superfusion under visual control was facilitated by the addition of 20 mM sucrose. The resulting increase in birefringence induced, as illustrated in Fig. 1, a clear definition of the boundaries of the stream, which, together with the micromanipulator-driven positioning of the tubes, permitted the exact placement of the superfusion. Because only a small part of the superfusion system was immersed in the experimental bath, the temperature of the superfusate as measured at the tip of the inlet tube was slightly (2–3°C) below bath temperature due to insufficient equilibration. Drugs applied during local superfusion included tetrodotoxin (TTX, Calbiochem, Luzern, Switzerland), nifedipine (Sigma, Buchs, Switzerland) and Bay K 8644 (kindly supplied by Dr. R. Gross, Bayer AG, Wuppertal, Germany).

Multiple-site optical recording of transmembrane voltage changes

The temperature-controlled experimental chamber containing the preparation was fixed on an inverted microscope equipped for epifluorescence (Axiovert 135 M, Zeiss, Switzerland), which was mounted on a custom-built X-Y-table. The table was driven by stepper motors either under manual control or with the aid of a computer-linked controller (MAC4000, Märzhäuser, Wetzlar, Germany), which offered a repositioning accuracy of ±3 μm. The light from a short-arc xenon lamp driven by a low-ripple power supply (Optiquip, NY) was, after passing a shutter (VS25S21 MO, Vincent Assoc., Rochester, NY), short-pass filtered (570 EFSP, Omega Optical, Brattleboro, VT) and deflected toward the objective by means of a dichroic mirror (575 nm, Omega Optical, Brattleboro, VT). Emitted fluorescence from the preparation was long-pass filtered (OG 590, Omega Optical, Brattleboro, VT) and projected onto a 2-dimensional array of 379 optical fibers, which formed a tightly packed hexagonal array. The diameter of each fiber was 1 mm resulting, e.g., along the horizontal center line, in a linear row of 21 detectors imaging the complete width of the field of view. With the typically used 20× objective (Fluar 20×, 0.75 NA, Zeiss, Zürich, Switzerland), each fiber gathered light emitted by a circular tissue area with a diameter of 50 μm. From the entire array, 80 fibers matching the shape of a given cell pattern were selected and connected to individual photodiodes. The resulting photocurrents were, after conversion to voltages by first-stage amplifiers, fed to sample-and-hold stages for subtraction of background fluorescence before they underwent final amplification (overall gain of 2.5 × 109 V/A). The bandwidths of all channels were fine-tuned to a rise time of 100 μs (f_0 = 1.7 kHz), thus permitting the accurate recording of impulse propagation at a microscopic level. The conditioned signals were simultaneously sampled at 20 kHz by a computer-based data acquisition system (Acer 486 DX-2, 66 MHz, Novitronic, Zürich, Switzerland, equipped with two 40-channel analog-to-digital converters, PCI 20501C, 12-bit; Burr Brown, Rüschlikon, Switzerland). The programs for the control of the experiments and the data acquisition were implemented in C (Borland C++ V4.0, Programmer's Paradise, Shrewsbury, NJ).

Fluorescent pictures of the preparations were taken with a videocamera (Sony, XC-77, Sony Corp., Paramus, NJ), which was connected to a monochrome framegrabber (Quickcapture, Data Translation Inc., Marlboro, MA) installed in a computer (Macintosh IIcx, Apple, Wallisellen, Switzerland) running an image acquisition program (Image, National Institutes of Health, Bethesda, MD). Even though pictures were taken using a reduction lens (0.5, Zeiss, Zürich, Switzerland), only 64% of the whole width of the field of view could be imaged by the CCD camera.

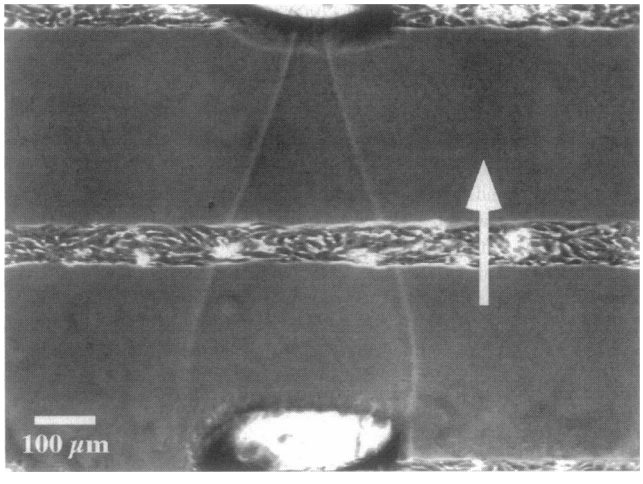

FIGURE 1 Phase contrast image (10× magnification) of an 80-μm wide cell strand being subjected to a local superfusion. The superfusate flows in the direction of the white arrow: it is ejected at a rate of 100 μl/min from the tube at the bottom of the picture and is subsequently withdrawn through the tube at the top, which operated at a rate of 1–2 ml/min. The lateral boundaries of the superfusion, which has an ellipsoid shape, can clearly be seen due to the birefringence induced by 20 mM sucrose added to the superfusion medium.

Data analysis

The raw data were analyzed by programming routines written in IDL (Interactive Data Language, Creaso GmBH, Gilching, Germany). The data processing typically involved manual selection of the upstroke portions of the action potentials to omit any signal distortion due to motion artifacts occurring several milliseconds after the upstrokes (Rohr and Salzberg, 1994b). The cropped traces were passed through a digital low-pass filter with a corner frequency of 1.5 kHz and the signal amplitudes obtained during retrograde stimulation under control conditions were set to 100%. All other measurements at a given location were scaled to this data set. We selected this particular set as an "anchor," because (i) it could be reasonably assumed that the maximal signal amplitudes during *retrograde* conduction were not significantly affected by the tissue geometry, and because (ii) phototoxicity and bleaching were not yet affecting the shape of the signal during this second in a row of six short illuminations (Rohr and Salzberg, 1994b). Assuming an average action potential amplitude (APA) of 100 mV (Rohr et al., 1991), the scaled values given as %APA translate directly into APA given in millivolts. Values for maximal upstroke velocities (dV/dt_{max}) were scaled correspondingly and are given as %APA/ms (making the assumption of an average APA of 100 mV under control conditions, %APA/ms corresponds to V/s). Activation times for each recording site were determined by averaging activation times obtained for 40% to 60% depolarization values in steps of 2% (Rohr and Salzberg, 1994b). From these values, both isochrones of activation and local and/or global conduction velocities (θ, cm/s) were calculated. Conduction delays due to geometrical expansions of the tissue were calculated as the difference between total antegrade and retrograde activation time across the whole field of view.

The effects of given interventions on APA, dV/dt_{max}, and θ were statistically evaluated by comparing values obtained during the intervention with the average of the control and washout values. This procedure, instead of a direct comparison to control values, was chosen to account for phototoxic effects, which, even though they were small, tended to depress all three parameters in a mostly linear fashion with the increasing number of illuminations during a given experiment.

Statistics

Values were compared using Student's *t*-test (two-tailed, homo- or heteroscedastic where appropriate) and differences were considered significant at $p < 0.05$.

RESULTS

Control superfusions of linear cell strands

In order to characterize the effects of the local superfusion per se on action potential amplitudes (%APA), maximal upstroke velocity (dV/dt_{max}, %APA/ms) and conduction velocities (θ, cm/s), we superfused defined regions of linear strands of cultured myocytes with a control solution consisting of regular bath medium containing 20 mM sucrose ($n = 14$). The experimental protocol was similar to that used during the experiments with abrupt tissue expansions, i.e., superfusion widths were 700 μm and the preparations were stimulated alternately from the left and from the right at a basic cycle length of 500 ms. The superfusion was placed such that only half of the cell strand measured optically was superfused while the other half served as control. Because the preparations exhibited homogeneous and symmetric conduction, the data of both directions of propagation were pooled. As listed in Table 1, the intervention slightly decreased both dV/dt_{max} (−6%) and conduction velocities (−8%) in the superfused segments. In contrast, it had virtually no effect on signal amplitudes (100 vs. 99% APA), dV/dt_{max} (97 vs. 95% APA/ms) and θ (35 vs. 35 cm/s) in the nonsuperfused regions, indicating that the visual control of the superfusion boundaries was effective and that the borders were stationary during the experiments. None of the depressions in the superfused segment, which were most likely due to the small temperature drop in the superfused region (see Methods), was significant when compared with the nonsuperfused segments. The possibility that the small increase in tonicity due to the added sucrose could have contributed to the effects of the superfusion is unlikely, based on a previous report (Bailey, 1981). This study showed that an even larger increase in tonicity (addition of 40 mM sucrose) had no significant effect on maximal resting membrane potential, action potential amplitude, dV/dt_{max}, and conduction velocity in canine Purkinje fibers.

Impulse propagation across an abrupt tissue expansion under control conditions

In all experiments, impulse propagation across tissue expansions was mapped with the spatial arrangement of fiber-optic sensors as shown in the upper sections of Fig. 2. This particular selection of sensors permitted (i) to record impulse propagation along the center line of the preparation at high spatial resolution (center-to-center distance of sensors: 50 μm) and (ii) to follow the two-dimensional spread of activation in the expansion with a slightly lower resolution (center-to-center distance of sensors: 100 μm). The dimensions of the preparations were chosen such that the length of the cell strand (1.8 mm) and the side lengths of the expansions (2.2 mm) largely exceeded published values for the space constant in monolayer cultures of neonatal rat heart cells (350 μm; Jongsma and van Rijn, 1972), thereby ensuring that the propagation characteristics were free of boundary effects at the site of the expansion. An example exhibiting successful bidirectional conduction and showing the typical features of propagation across an abrupt expansion of excitable tissue is shown in Fig. 2. The preparation, which consisted of a 30-μm wide cell strand connected to a large rectangular cell area, was stimulated both in antegrade (*A*) and the retrograde direction (*B*). During antegrade activation, propagation was fast and continuous in the cell strand before slowing down at the site of the expansion. As illustrated by the isochrones, activation proceeded radially into the monolayer, picking up speed with increasing distance from the site of the expansion. The slowing of propagation at the site of the expansion during antegrade conduction was accompanied by typical changes of the shape of the action potential upstroke as measured along the center line of the preparation (recording sites indicated by *open circles*): due to electrotonic interactions, an increasingly reduced initial plateau height proximal to the expansion was followed by double-hump-upstrokes at the geometrical transition and prominent footpotentials up to 200 μm into the expansion. In contrast, during retrograde conduction, the activation wavefront was planar, crossed the geometrical contraction in a continuous fashion and accelerated in the narrow cell strand ($\theta_{expansion}$ 29 cm/s; θ_{strand} 52 cm/s). The temporal difference between antegrade and retrograde activation in this particular preparation amounted to 1.3 ms. This delay could be entirely attributed to the current-to-load mismatch, because retrograde conduction did not show any discontinuities indicating longitudinal resistance problems.

Local block of I_{Na} proximal to abrupt expansions with TTX

Because I_{Na} is the major inward current in ventricular myocardium, it could be expected that a block of this current in the tissue proximal to the expansion would induce UCB due to the aggravation of the current-to-load mis-

TABLE 1 Effects of local superfusion with control solution (linear cell strands)

	n	Strand diameter (μm)	Superfusion width (μm)	Superfusion duration (min)	Signal amplitude (% APA) avcw*	Signal amplitude (% APA) Superfusion	dV/dt_{max} (% APA/ms) avcw	dV/dt_{max} (% APA/ms) Superfusion	θ (cm/s) avcw	θ (cm/s) Superfusion
Superfused segment	14	57 ± 5	700 ± 0	3.0 ± 0	99 ± 3	101 ± 5	97 ± 12	92 ± 12	32 ± 6	29 ± 6
Nonsuperfused segment	14	57 ± 5	—	—	100 ± 3	99 ± 5	97 ± 12	95 ± 12	35 ± 6	35 ± 7

*avcw: Average of control and washout data.

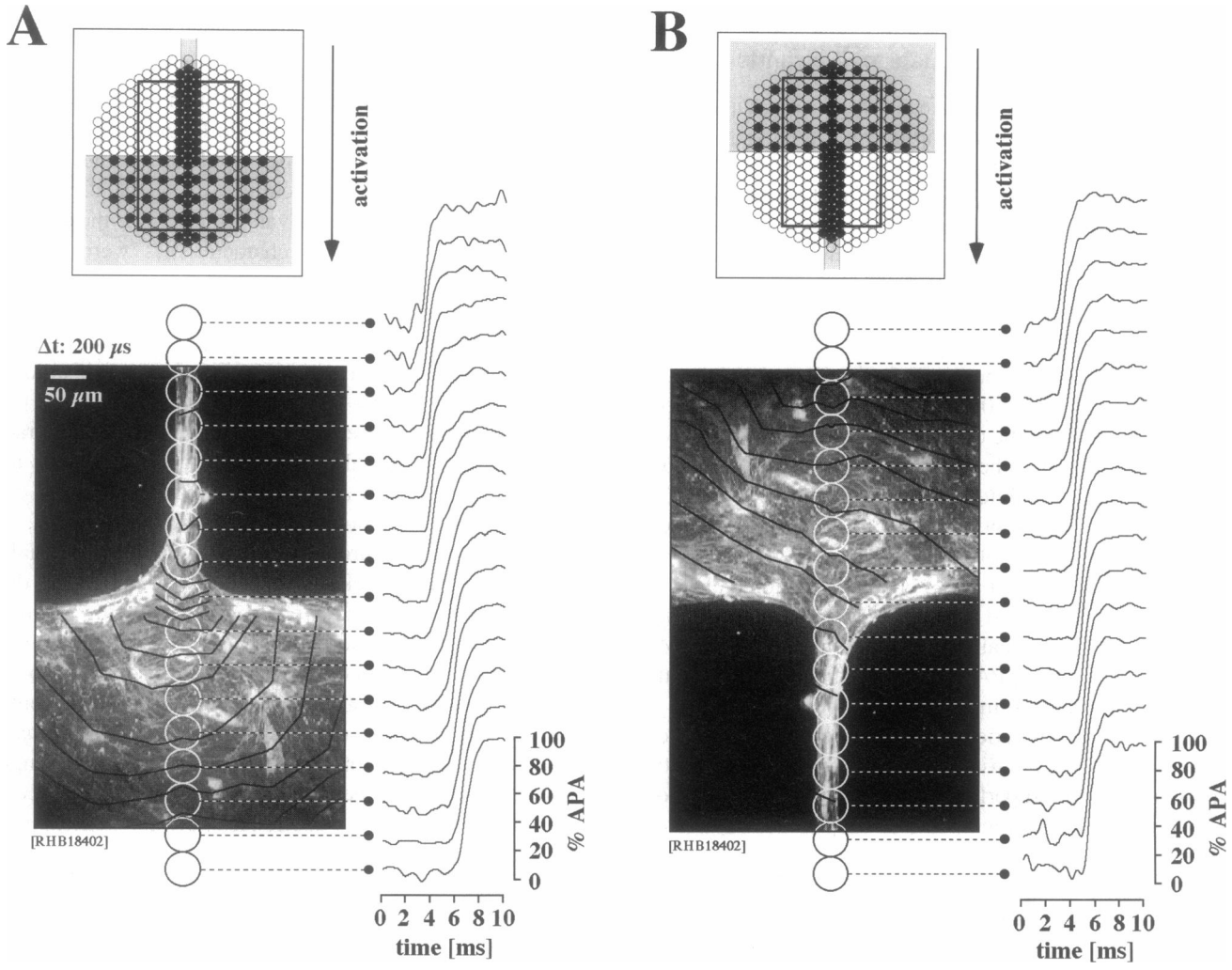

FIGURE 2 Successful bidirectional impulse propagation across an abrupt expansion of excitable tissue under control conditions. (*A*, *upper section*) Schematic drawing depicting the shape and orientation of the preparation (*gray expansion*) in respect to the fiberoptic array (each *circle* represents a single fiber, with *filled circles* indicating actual recording locations). The black rectangle in the fiberoptic array outlines the size and position of the picture taken with the CCD camera. (*A*, *lower section*) Impulse propagation in the antegrade direction: the fluorescence microphotograph shows the preparation, which consisted of a 30-μm-wide cell strand connected to a large rectangular cell monolayer. Overlaid on the picture are, in black, isochrones of activation (interval = 200 μs) and, in white, positions of a subset of photodetectors. Action potential upstrokes as recorded by this subset are shown to the right of the microphotograph. During antegrade stimulation activation was slowed at the expansion and became curved as it invaded the large rectangular cell monolayer. In this particular example the conduction delay amounted to 1.3 ms, and action potential upstrokes recorded in the region giving rise to the delay displayed typical "double-hump" distortions (for explanation see text). (*B*, *upper section*) c.f. explanation for the same section in (*A*). (*B*, *lower section*) Impulse propagation in the retrograde direction: according to the reversed direction of activation, the layout is rotated by 180°. In contrast to antegrade activation, the wavefront during retrograde activation was planar and invaded the narrow cell strand without any delays, as illustrated both by the regular spacing of the isochrones and the monophasically rising action potential upstrokes. In the strand itself, propagation velocity increased.

match. This prediction was tested in five preparations, where the narrow cell strands, having a width of 36 ± 5 μm, were superfused along a distance of 480 ± 160 μm (range 300–700 μm) with 10 μM TTX. For these experiments, we selected preparations with small antegrade conduction delays across the expansion under control conditions (0.96 ± 0.25 ms), i.e., preparations in which the expansion had a relatively small effect on antegrade conduction. The results obtained in one preparation are shown in Fig. 3. Under control conditions, propagation was successful in both directions with a barely visible antegrade conduction delay of 0.9 ms across the expansion. Superfusion of the thin cell strand with TTX for a length of 600 μm in front of the expansion (undulating waves in schematic drawing of the preparation) induced an antegrade conduction block, while retrograde conduction was still successful, showing, in the superfused region, a decrease of dV/dt_{max} from 115 to 43% APA/ms and a slowing of conduction from 49 to 19 cm/s. The decrease in dV/dt_{max} could also be noted in the superfused segment during antegrade conduction, where it was, however, mixed with a slowing of the upstroke accompanying decremental conduction. As shown in the rightmost panel of Fig. 3, all of the changes induced by TTX were fully reversible upon washout. The same results were ob-

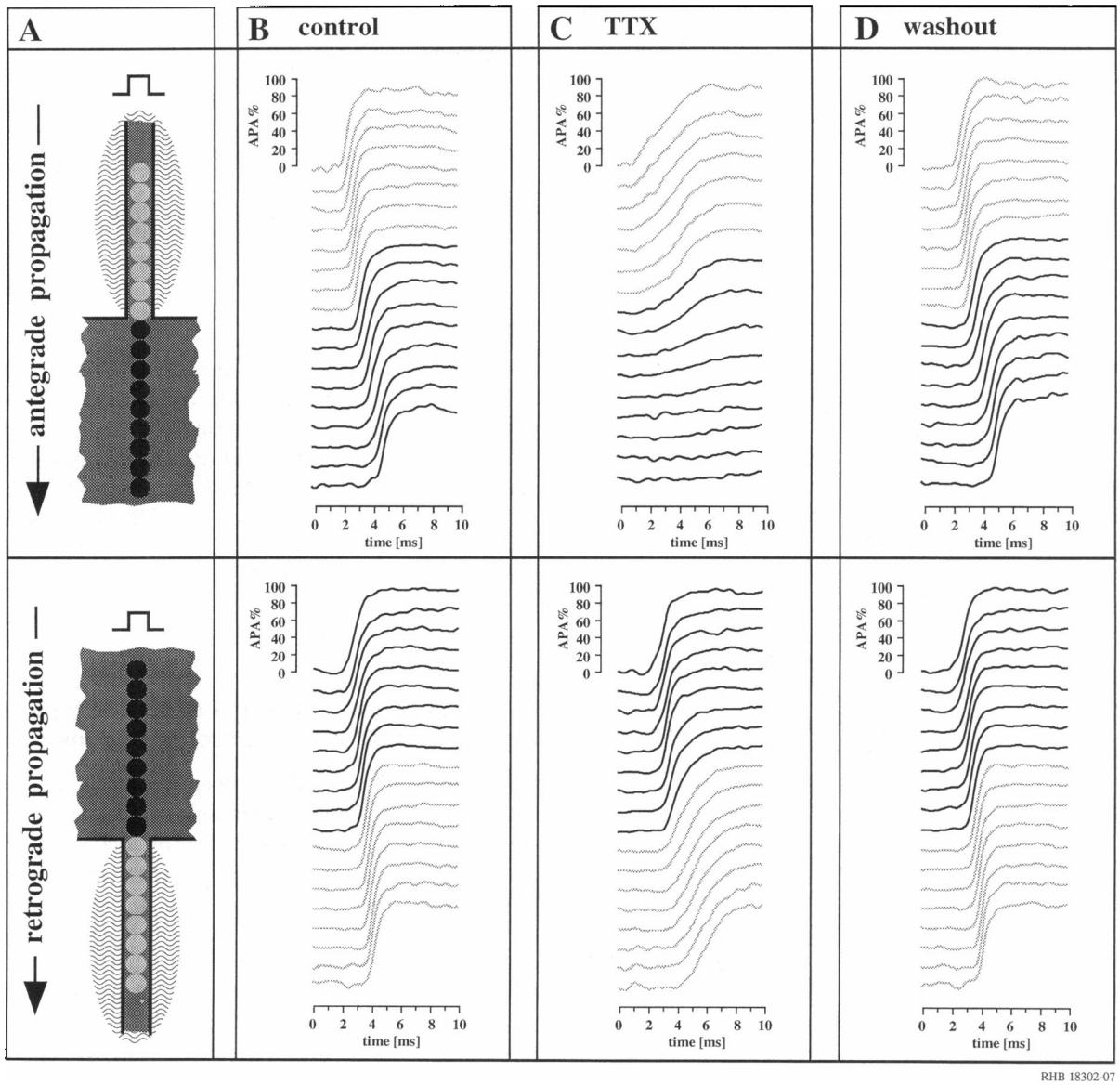

FIGURE 3 Effect of block of I_{Na} confined to the cell strand on bidirectional impulse propagation across an abrupt tissue expansion. (*A*) Schematic drawing of the preparation (*dark gray*), which consisted of a 40-μm-wide cell strand connected to a rectangular cell monolayer measuring 2.2 mm × 2.2 mm; the overlaid disks (*light-gray* along the strand and *black* in the expansion) correspond to the locations where action potentials were recorded optically (signals are coded correspondingly in *black* and *gray*), and the undulating waves indicate the position and extent of the local superfusion with 10 μM TTX (600 μm wide). The orientation of the schemes are changed according to the site of stimulation (*upper scheme*: antegrade; *lower scheme*: retrograde). (*B*) Under control conditions antegrade activation (*upper set of traces*) invaded the expansion with a very small delay of 0.9 ms. Because of this small delay, the upstrokes of the action potentials recorded at the site of expansion were not distorted, i.e., they rose in a monophasic manner. Following retrograde stimulation (*lower set of traces*), activation proceeded unhindered through the preparation. (*C*) During local superfusion of the narrow cell strand with TTX, antegrade propagation failed to invade the expansion. Compared with control, upstroke velocities were significantly reduced and signal amplitudes were progressively smaller due to the electrotonic interaction with the nonactivated tissue expansion. After retrograde stimulation the activation proceeded unhindered through the preparation. However, both dV/dt_{max} and conduction velocities were significantly reduced in the superfused segment. (*D*) After washout for 5 min, the effects induced by TTX were completely reversed except for a small increase in the antegrade conduction delay to 1.1 ms.

tained in the remaining four preparations. The general effects of the local TTX superfusion on signal amplitudes, dV/dt_{max} and conduction velocity as assessed during successful retrograde conduction, are listed in Table 2. While TTX only slightly reduced the amplitudes (−2%, ns), it induced significant decreases of both dV/dt_{max} (−61%; $p < 0.001$) and conduction velocity (−59%; $p < 0.001$).

Local block of I_{Ca} proximal to abrupt expansions with nifedipine

If I_{Ca}, in addition to I_{Na}, were to be considered an important contributor to the total inward current in the setting of a current-to-load mismatch, a reduction of this current should, in analogy to a reduction of I_{Na}, favor the occurrence of

TABLE 2 Effects of local superfusion with 10 μM TTX (expansions)

					Retrograde Conduction						Antegrade Conduction	
					Signal amplitude (% APA)		dV/dt_{max} (% APA/ms)		θ (cm/s)		Delay (μs)	
	n	Strand diameter (μm)	Superfusion width (μm)	Superfusion duration (min)	avcw	Superfusion	avcw	Superfusion	avcw	Superfusion	Control	Superfusion
superfused segment	5	36 ± 5	480 ± 160	3.5 ± 0.7	97 ± 3	95 ± 8	109 ± 8	42 ± 8*	53 ± 4	21 ± 2*	960 ± 245	block

avcw: Average of control and washout data.
*Significant difference versus control.

UCB across abrupt tissue expansions. To test this hypothesis, thin cell strands of 15 preparations were superfused for a length of 770 μm ± 60 μm (range: 700–900 μm) in front of the expansion with 5 μM nifedipine. This concentration of nifedipine induced complete cessation of contractile activity in the region undergoing superfusion. An example of a preparation in which this intervention induced UCB is shown in Fig. 4. Under control conditions, propagation was successful in both directions with an antegrade conduction delay of 1.9 ms across the expansion and unhindered retrograde conduction. Superfusion of the thin cell strand for a length of 800 μm in front of the expansion (undulating waves in schematic drawing of the preparation) induced an antegrade conduction block, while retrograde conduction was virtually unaffected (transient decrease of total retrograde conduction time of less than 5%). After washout for 5 min, control conditions were restored with the exception of a minimal increase of the antegrade conduction delay across the expansion. This residual effect was commonly observed both in blocking and nonblocking preparations and was, although an insufficient washout cannot be ruled out, most probably attributable to the onset of phototoxic effects due to the repeated illuminations (total of six recordings at the same location). In all of the 15 preparations tested, nifedipine elicited UCB in 9 cases, which were fully reversible upon washout. In the remaining six preparations the superfusion failed to induce UCB, but increased, in a significant and reversible manner, the antegrade conduction delay across the expansion from 0.94 ± 0.15 ms to 1.89 ± 0.39 ms ($p = 0.004$). As further detailed in Table 3, the two groups of preparations were, under control conditions, similar both in respect to their geometrical and functional parameters with the only significant difference concerning the antegrade conduction delay across the expansion, which amounted to 1.65 ± 0.88 ms in the cases of preparations exhibiting UCB, and 0.94 ± 0.15 ms in the cases where nifedipine failed to induce UCB ($p = 0.04$). Based on all values, the antegrade conduction delay being decisive for induction of UCB was 1.0 ms; preparations with smaller delays showed UCB in only one of six cases; whereas, in preparations with larger delays, UCB could be elicited in eight of nine cases.

In general, the superfusion of the thin cell strand with 5 μM nifedipine induced, as observed during retrograde propagation in all 15 experiments, a small but significant reduction of all of the parameters measured (APA: −10%; dV/dt_{max}: −12%; θ: −6%; see Table 3). Because it could not be entirely ruled out that these transient decreases, which were most likely due, at least in part, to the superfusion induced small drop in local temperature (see Methods), were themselves involved in the induction of UCB due to a reduction of I_{Na} (Downar and Waxman, 1976), we performed a series of complementary experiments in which an augmentation of I_{Ca} was expected to reverse preexistent UCBs.

Local boost of I_{Ca} proximal to abrupt expansions exhibiting UCB under control conditions

While, generally, impulse propagation was successful in both directions across abrupt tissue expansions, some preparations displayed UCB under control conditions owing to current-to-load mismatch. These preparations were used to test the hypothesis that an increase of I_{Ca} in the cell strand adjacent to the expansion would reestablish successful bidirectional conduction. To this purpose, 700-μm-wide segments of the thin cell strands adjacent to the expansions were superfused with 1 μM Bay K 8644 for up to 3 min. The results obtained in one experiment exhibiting break-up of UCB during this intervention is shown in Fig. 5. The preparation consisted of a narrow cell strand with a diameter of 50 μm connected to a large rectangular tissue area. Under control conditions, antegrade propagation failed at the expansion, while retrograde conduction invaded the whole preparation in a continuous manner, thereby indicating that the UCB was entirely due to the current-to-load mismatch represented by the expansion. During superfusion of the cell strand with 1 μM Bay K 8644, antegrade UCB was overcome, while retrograde conduction was slowed by 12% in the superfused area. Successful antegrade propagation in the presence of Bay K 8644 was characterized by an overall conduction delay across the expansion of 3.9 ms and, compared with control and washout, by a decreased rate of initial repolarization, which was especially pronounced in the region adjacent to the expansion. This prolonged plateau was most likely a direct effect of the Bay K 8644-induced stimulation of I_{Ca}. Washout caused a prompt reversal of all observed effects. In four of six preparations exhibiting UCB under control conditions, superfusion of the thin cell strand with Bay K 8644 resulted in the establishment of successful

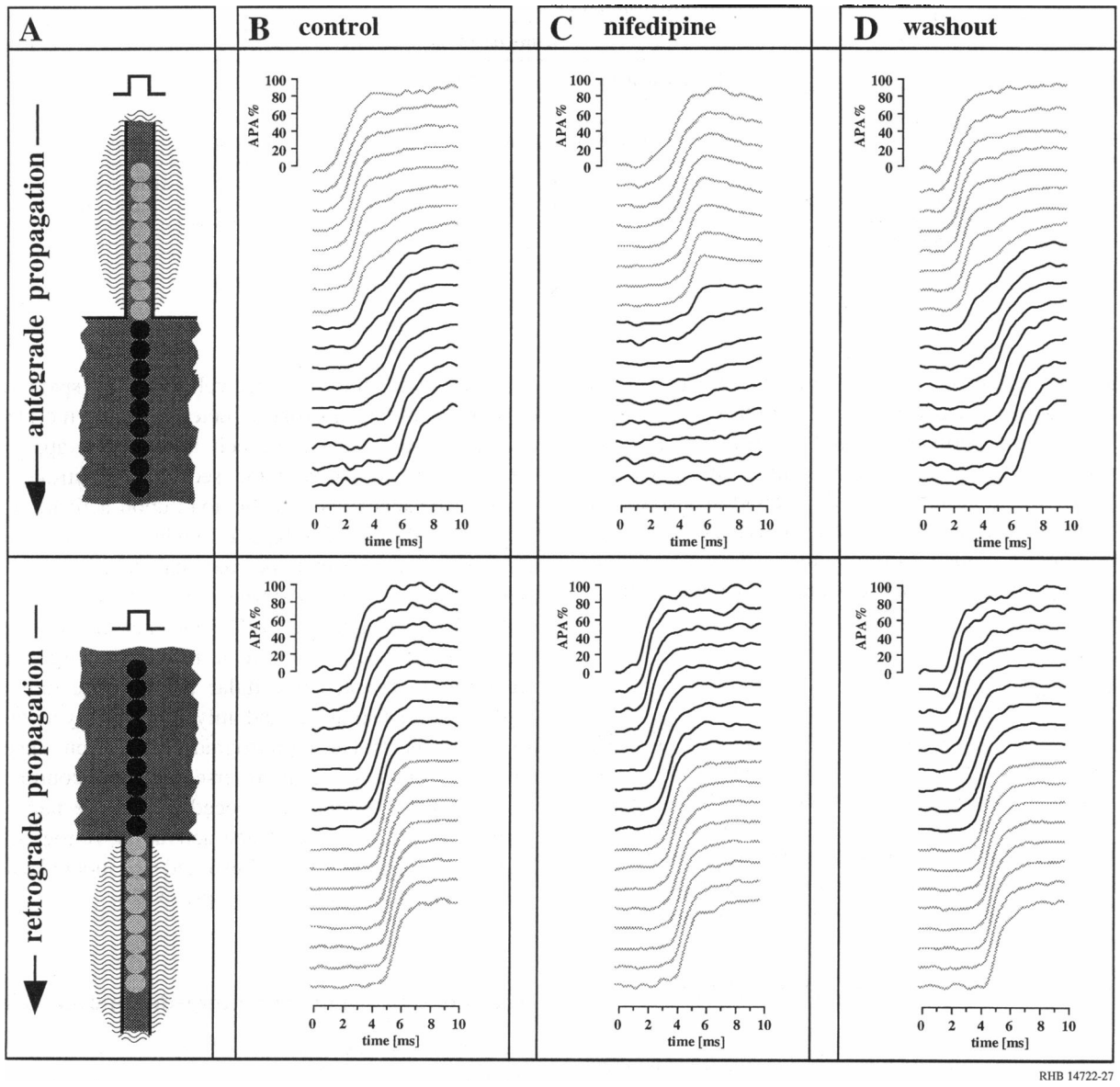

FIGURE 4 Induction of UCB by application of nifedipine to the cell strand adjacent to the expansion. (*A*) Schematic drawing of the preparation (*dark gray*), which consisted of a 40-μm-wide cell strand connected to a rectangular cell monolayer measuring 2.2 mm × 2.2 mm; the overlaid disks (*light-gray* along the strand and *black* in the expansion) correspond to the locations where action potentials were recorded optically (signals are coded correspondingly in *black* and *gray*), and the undulating waves indicate the position of the local superfusion with 5 μM nifedipine (800 μm wide). The orientation of the schemes are changed according to the site of stimulation (*upper scheme*: antegrade; *lower scheme*: retrograde). (*B*) Under control conditions, antegrade activation (*upper set of signals*) invaded the expansion with a delay of 1.9 ms. Typically, action potential upstrokes in the close vicinity of the expansion were biphasic, displaying marked double-humps at the expansion itself. After retrograde stimulation (*lower set of upstrokes*), activation proceeded unhindered through the preparation. (*C*) During local superfusion of the narrow cell strand with nifedipine, antegrade impulse propagation failed to invade the expansion, as illustrated by the progressively smaller signal amplitudes due to the electrotonic interaction with the nonactivated tissue expansion. During retrograde stimulation (*lower set of signals*), activation proceeded unhindered through the preparation and was indistinguishable from control, both in terms of upstroke velocities and conduction velocities. (*D*) After washout for 5 min, the effects induced by nifedipine were completely reversed.

bidirectional conduction with an average antegrade conduction delay across the expansion of 3.6 ± 1.7 ms. This effect was fully reversible after 5 min of washout. Qualitatively similar results were obtained in an additional seven experiments, where the thin cell strands were superfused for a length of 800 μm with a reduced concentration of Bay K 8644 (100 nM) for up to 3.5 min. This lower concentration of Bay K 8644 was still effective in reversing UCB. However, as expected for a smaller stimulation of I_{Ca}, the percentage of UCB reversals (three of seven) was smaller, and the average antegrade conduction delay across the expansion during reestablishment of bidirectional conduction was longer (5.2 ± 2.2 ms) than that obtained with 1 μM Bay K 8644.

The effects of the intervention as assessed during control retrograde propagation in the superfused strand segment are

TABLE 3 Effects of local superfusion with nifedipine (expansions)

UCB induction	n	Strand diameter (μm)	Superfusion width (μm)	Superfusion duration (min)	Retrograde Conduction: Signal amplitude (% APA) avcw	Signal amplitude (% APA) Superfusion	dV/dt_{max} (% APA/ms) avcw	dV/dt_{max} (% APA/ms) Superfusion	θ (cm/s) avcw	θ (cm/s) Superfusion	Antegrade Conduction: Delay (μs) Control	Delay (μs) Superfusion
yes	9	42 ± 8	760 ± 50	2.3 ± 1.0	98 ± 4	88 ± 4*	109 ± 31	96 ± 30*	37 ± 4	35 ± 5*	1650 ± 880	block
no	6	33 ± 11	800 ± 60	3.2 ± 0.4	97 ± 3	91 ± 3*	125 ± 18	115 ± 18*	40 ± 8	37 ± 7*	940 ± 150[£]	1890 ± 390*

avcw: Average of control and washout data.
*Significant difference avcw versus superfusion.
[£]Significant difference UCB versus non-UCB.

summarized in Table 4. Irrespective of the effect on UCB, the superfusion with 1 μM Bay K 8644 induced, in contrast to the nifedipine experiments, a slight increase of the signal amplitude (up to +5%), which was most likely a direct consequence of the stimulation of I_{Ca} supporting an elevated action potential plateau. Conversely, superfusion with Bay K 8644 induced, similar to nifedipine, a decrease of both dV/dt_{max} (up to −7%) and conduction velocity (up to −10%).

DISCUSSION

It has previously been shown in cardiac tissue that the success of impulse propagation in the setting of a current-to-load mismatch as represented by an abrupt tissue expansion is dependent on the geometry of the expansion and on the size of I_{Na}. With the present study, we extend these results by the finding that the success of antegrade propagation across a tissue expansion can also depend on I_{Ca}.

Impulse conduction characteristics of the model system

Similar to the Purkinje fiber ventricular junction in intact cardiac tissue (Mendez et al., 1970; Veenstra et al., 1984), impulse propagation from a thin cell strand (current source) to a large expansion (current sink) in patterned growth monolayer cultures of myocytes can be locally delayed at the site of expansion. The magnitude of this delay is a function of the shape of the expansion (funneled, rectangular, incised), as well as of the diameter of the cell strand proximal to the expansion. Depending on these parameters, antegrade propagation is delayed by up to several milliseconds at the expansion, or, below a critical diameter of the cell strand, UCB can occur (Rohr and Salzberg, 1994a; Fast and Kléber, 1995a). Typically (cf. Fig. 2), action potential upstrokes during delayed antegrade conduction are monophasic both in the thin cell strand and in the large rectangular cell monolayer, while, in the close vicinity of the expansion, they are distorted by bidirectional electrotonic interactions across the expansion: an initial, gradually diminishing and progressively slower rising upstroke is, after a small intermediate plateau, followed by a secondary, increasingly larger and faster rising upstroke as the wavefront progresses into the large cell area. The spatial evolution of the initial upstroke is determined by the electrical load imposed by the large cell area on the approaching action potential, whereas the secondary upstroke results from the disappearance of this load upon activation of the large area (Rohr and Salzberg, 1994a). The isochrones of activation illustrate that the maximal delay occurs in the expansion (Leon and Roberge, 1991; Rohr and Salzberg, 1994a; Fast and Kléber, 1995b) and that the wavefront of activation becomes circular as it invades the large cell area according to the actual cellular microarchitecture of the expansion consisting of randomly oriented myocytes (isotropic cell sheet). During retrograde stimulation, the activation wavefront is planar, transverses the tissue contraction in an unhindered fashion, and speeds up in the narrow cell strand. In contrast to antegrade activation, retrograde conduction is continuous, as illustrated by monophasic and evenly spaced action potential upstrokes.

Frequency of tissue geometry-dependent UCB

In contrast to earlier findings (Rohr and Salzberg, 1994a), where we could not observe structurally fixed UCB even if the narrow cell strands were only one- to two-cells wide, such blocks were abundant in the preparations used in the present experiments. Also, we observed UCB at larger strand diameters (up to 60 μm) than those reported earlier by Fast et al. as being critical for induction of UCB (15 μm; Fast and Kléber, 1995a). These discrepancies with earlier findings are most likely due to altered culture conditions: in the present experiments the culture medium was supplemented for the first 2–3 days with 10 μM epinephrine. This drug is expected to have two effects: first, it increases the cell size due to its α_1-adrenergic action (Simpson, 1985) and, therefore, enhances the tight apposition of the cells in culture. Secondly, the resulting increase in cAMP is likely to induce an increased expression of gap junctions (Darrow et al., 1996). Both of these effects favor the occurrence of UCB because they increase the electrical load represented by the expansion by increasing the capacitance (enlarged cells) and by enhancing the degree of electrical coupling (Fast and Kléber, 1995b).

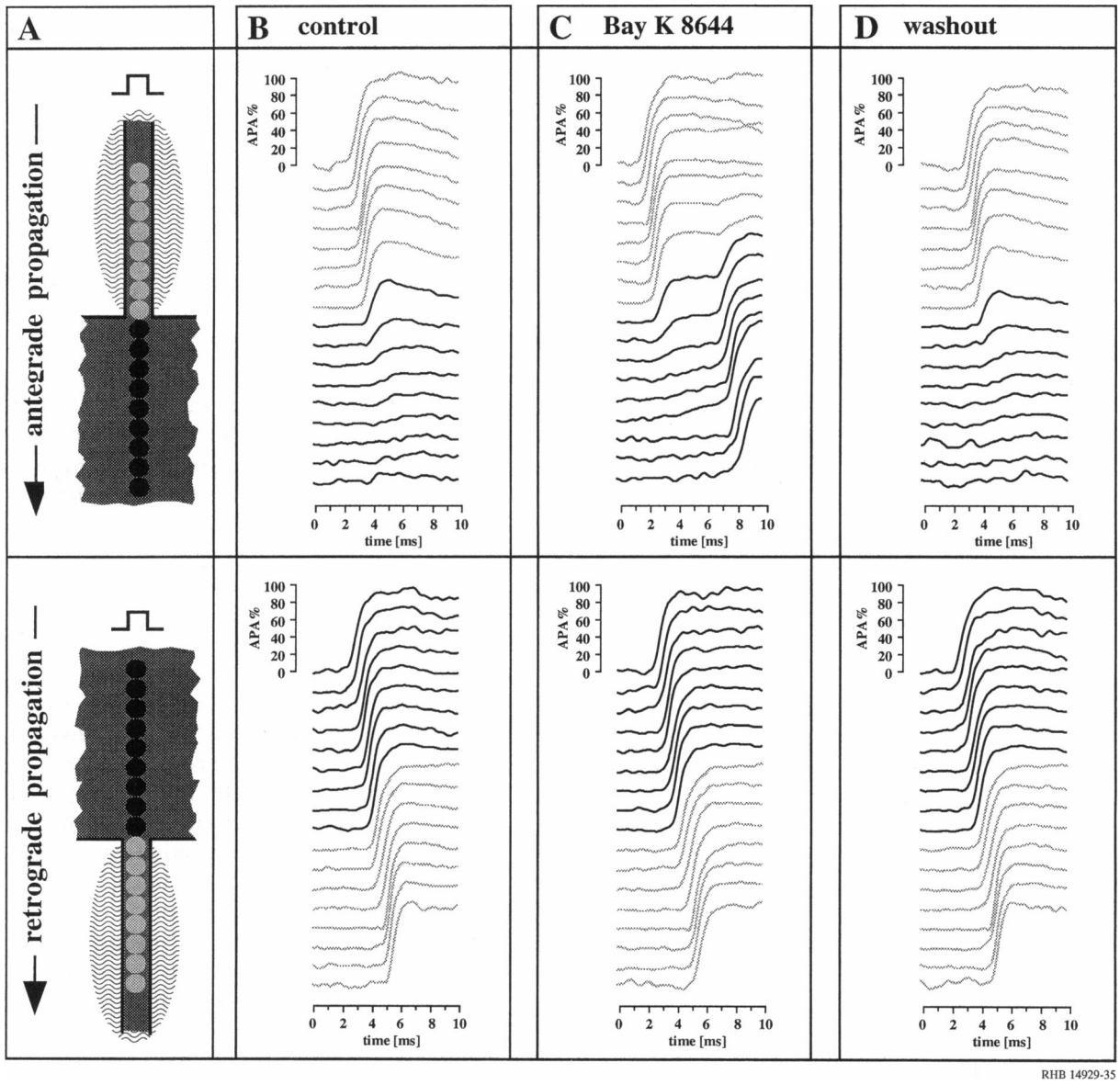

FIGURE 5 Conversion of UCB into successful conduction during enhancement of I_{Ca} in the cell strand adjacent to the expansion with Bay K 8644. (*A*) Schematic drawing of the preparation (*dark gray*), which consisted of a 50-μm-wide cell strand connected to a rectangular cell monolayer measuring 2.2 mm × 2.2 mm; the overlaid disks (*light-gray* along the strand, *black* in the expansion) correspond to the locations where action potentials were recorded optically (signals are coded correspondingly in *black* and *gray*) and the undulating waves indicate the position of the local superfusion with 1 μM Bay K 8644 (700 μm wide). The orientation of the schemes is changed according to the site of stimulation (*upper scheme*: antegrade; *lower scheme*: retrograde). (*B*) under control conditions, antegrade activation (*upper set of upstrokes*) failed to invade the expansion, as illustrated by the progressively smaller signal amplitudes due to the electrotonic interaction with the nonactivated tissue expansion. After retrograde stimulation (*lower set of upstrokes*), activation proceeded unhindered through the preparation. (*C*) During local superfusion of the narrow cell strand with Bay K 8644, antegrade activation successfully invaded the expansion with a conduction delay of 3.9 ms. Retrograde activation (*lower set of signals*) proceeded unhindered through the preparation. (*D*) After a washout period of 5 min, UCB was reestablished.

Role of I_{Na} in the setting of a current-to-load mismatch

In addition to geometrical considerations, the success of impulse propagation across abrupt expansions is dependent on the size of the inward current delivered by the current source. In this respect, it has previously been shown in Purkinje fiber-ventricular preparations that a depression of I_{Na}, either by elevation of extracellular potassium (Mendez et al., 1970; Overholt et al., 1984) or by direct reduction with procaine (Matsuda et al., 1967), induced UCB. The same effect could invariably be elicited in our preparations by blocking I_{Na} in the thin cell strand proximal to the expansion with 10 μM TTX. The formation of UCB in these preparations was independent of the size of the antegrade conduction delay under control conditions (0.6–1.3 ms), and superfusion widths as small as 300 μm, i.e., in the range

TABLE 4 Effects of local superfusion with Bay K 8644 (expansions)

UCB reversal	n	Strand diameter (μm)	Bay K 8644 concentration (μM)	Superfusion width (μm)	Superfusion duration (min)	Retrograde conduction: Signal amplitude (% APA) avcw	Retrograde conduction: Signal amplitude (% APA) Superfusion	Retrograde conduction: dV/dt_{max} (% APA/cm) avcw	Retrograde conduction: dV/dt_{max} (% APA/cm) Superfusion	Retrograde conduction: θ (cm/s) avcw	Retrograde conduction: θ (cm/s) Superfusion	Antegrade conduction: Delay (μs) Control	Antegrade conduction: Delay (μs) Superfusion
yes	4	45 ± 6	1.0	700	2.8 ± 0.5	97 ± 2	101 ± 4*	102 ± 6	95 ± 5*	30 ±2	27 ± 1*	block	3580 ± 1730
no	2	45 ± 14	1.0	700	3.0 ± 0	98 ± 0	103 ± 1*	105 ± 8	105 ± 3	36 ± 2	34 ± 1	block	block
yes	3	50 ± 9	0.1	800	3.3 ± 0.3	94 ± 3	95 ± 4	84 ± 7	87 ± 9	48 ± 11	43 ± 7	block	5200 ± 2210
no	4	43 ± 13	0.1	800	3.0 ± 0	98 ± 2	101 ± 5	98 ± 6	95 ± 7	49 ± 4	45 ± 4	block	block

avcw: Average of control and washout data.
*Significant difference versus control.

of a single space constant (Jongsma and van Rijn, 1972), were effective inducers of UCB. During retrograde conduction, even though the segment superfused with TTX displayed significant reductions of both dV/dt_{max} and conduction velocity, propagation never failed. This is in agreement both with our own observation that TTX failed to induce conduction block in linear cell strands (Rohr et al., 1996), and with earlier reports describing successful conduction in the presence of 5–16 μM TTX in linear excitable tissue structures, such as papillary muscles from guinea pigs or rabbits (Osaka et al., 1989; Ozaki et al., 1989). It suggests that the induction of UCB with TTX in the present experiments was entirely dependent on the current-to-load mismatch represented by the abrupt tissue expansion.

Induction of UCB with nifedipine

In contrast to the TTX experiments, which invariably induced antegrade conduction failure across expansions, the probability of induction of UCB with nifedipine was determined by the size of the antegrade conduction delay across a given expansion under control conditions. Delays larger than 1.0 ms favored the induction of UCB by nifedipine, while, in the case of smaller delays, antegrade conduction rarely failed. This critical value of 1.0 ms is in the range of previously reported values for time-to-peak of I_{Ca} (1–3 ms for L-type calcium current measured at 35° to 37°C; Isenberg and Klöckner, 1982; Mitchell et al., 1983; Cavalié et al., 1985; Luo and Rudy, 1994; Jeffrey and Allen, 1996) and therefore is in accordance with an involvement of I_{Ca} in the impulse conduction process across tissue expansions. The contribution of I_{Ca} to successful antegrade activation was, furthermore, directly visible by comparing the time course of the transmembrane potential immediately following the initial fast upstroke (cf. signals in the cell strand during antegrade conduction in the absence (Fig. 4 *B*) and presence (Fig. 4 *C*) of nifedipine): in the absence of nifedipine), i.e., during successful antegrade conduction, transmembrane potentials continued to depolarize at a slow rate during the conduction delay, whereas during the nifedipine-induced block, potentials started to repolarize immediately during the same time span. This difference suggests that I_{Ca} contributed the additional excitatory current needed to sustain the intermediate plateau at the peak of the initial upstroke and, as a consequence, successful antegrade conduction. In contrast to the effects of nifedipine on antegrade conduction, conduction in the retrograde direction remained unhindered. This was to be expected because I_{Ca} peaked with the above-mentioned latency in the range of a millisecond and, therefore, was too slow to contribute excitatory inward current to the leading edge of the activation wavefront during fast and continuous impulse propagation.

The importance of I_{Ca} for successful action potential transfer under conditions of very long activation delays has previously been demonstrated in pairs of individual myocytes coupled by a high extrinsic coupling resistor (Sugiura and Joyner, 1992) and, recently, in single myocytes coupled, in realtime, to a computer model of a ventricular cell (Joyner et al., 1996). In these experiments, exposure to 1 μM nifedipine lengthened, at high coupling resistances, the action potential transfer delay between the two cells (or the cell and the computer model) and reduced the maximal coupling resistance still supporting successful action potential transfer. While these results, similar to our findings, stress the importance of I_{Ca} in the process of delayed activation, delays under control conditions had to be much longer (>5 ms) than those found in the present study (>1 ms) before nifedipine effects became discernible. While this difference might have been due to the different nifedipine concentrations used (1 μM vs. 5 μM in the present study) or to species-dependent differences, it nevertheless raises the question whether the action potential transfer in the two-cell model (TCM) has a different sensitivity toward a reduction of I_{Ca} than impulse conduction across abrupt tissue expansions. In this respect, a major difference between the two experimental systems consists in the degree of electrical loading of the current source: because of the low intercellular conductances used in the TCM studies (≤15 nS for nifedipine effects to occur; Joyner et al., 1996), loading of the source can be expected to be considerably smaller than that occurring in cell cultures (48 nS between cultured pairs of neonatal rat ventricular myocytes; Bukauskas and Weingart, 1993). As a consequence of this higher electrical loading of the cell strand proximal to the expansion, the rate of early repolarization of the current source should, in comparison to TCMs, be increased, thereby unmasking the

contribution of I_{Ca} to the propagation process at an earlier time after the initiation of the action potential.

Relief of UCB with Bay K 8644

Because the superfusion per se slightly decreased dV/dt_{max} and conduction velocity, it could be argued that induction of UCB by nifedipine was not entirely specific, but was partly due to these superfusion-dependent effects. To exclude this possibility, we selected preparations exhibiting UCB under control conditions with the aim of reestablishing bidirectional conduction during an increase of I_{Ca} with Bay K 8644 (Cohen and Lederer, 1987). The I_{Ca} agonist reestablished bidirectional conduction in four of six cases at a concentration of 1 μM, and in three of seven cases at a concentration of 100 nM. Successful antegrade conduction during Bay K 8644 superfusion was characterized by relatively long delays across the expansion (3.6 ms and 5.2 ms, respectively) and the appearance of a "holding" potential at the peak of the initial depolarization at a given site before activation of the expansion occurred (cf. Fig. 5 *C*). Obviously, the current supporting the holding potential, which ultimately led to the success of propagation, was supplied by the Bay K 8644-induced increase in calcium inward current.

While the reciprocal results obtained with both nifedipine and Bay K 8644 suggest the direct involvement of I_{Ca} in the determination of the success of propagation across an abrupt tissue expansion, these compounds, which belong to the class of dihydropyridines, are known to have qualitatively similar effects on I_{Na} and I_{Ca} (Yatani and Brown, 1985; Yatani et al., 1988; Sugiura and Joyner, 1992; Beyer et al., 1994). One might therefore argue that the effects observed with the two compounds could be due, at least in part, to their action on the sodium channels. While we cannot rule out this possibility for nifedipine, which induced small but significant reductions in both dV/dt_{max} and conduction velocity, the results obtained with Bay K 8644 are clearly at odds with such an explanation. In the preparations where UCB was overcome during the superfusion with 1 μM Bay K 8644, this drug induced reductions of dV/dt_{max} and conduction velocity during retrograde conduction that were similar to those observed during superfusion with nifedipine. Thus, an enhancement of I_{Na} by Bay K 8644 was highly unlikely, suggesting that both of the effects, induction of UCB with nifedipine and relief of UCB with Bay K 8644, were due to the modulation of I_{Ca}.

The results obtained with both nifedipine and Bay K 8644 demonstrate, in a qualitative fashion, that I_{Ca} is involved in the success of impulse propagation in the setting of a current-to-load mismatch. The analysis of quantitative aspects of this effect might profit from the use of computer models of propagation across expansions of excitable tissue (Goldstein and Rall, 1974; Leon and Roberge, 1991; Fast and Kléber, 1995a; Fast and Kléber, 1995b), which would incorporate recent formulations of the dynamics of I_{Ca} (Luo and Rudy, 1994).

Relevance of the findings for impulse propagation in ventricular tissue

The data presented suggest that the calcium inward current is, in the continued presence of the sodium current, involved in the success of conduction across abrupt tissue expansions. This finding, together with the observation of an involvement of I_{Ca} in successful conduction between two partially uncoupled cells (Sugiura and Joyner, 1992), suggest that I_{Ca} might be essential for successful propagation in any situation where a local activation delay of sufficient length allows I_{Ca} to sustain depolarized transmembrane potentials, thereby increasing excitatory current flow to the distal cells. Such situations are likely to be present, e.g., in the border zone of a healing infarct (Ursell et al., 1985), where the complex architecture of the surviving tissue might comprise abruptly expanding cell structures resembling those modeled in culture in the present study. In this situation, application of a calcium channel antagonist might induce UCB, thereby preparing the grounds for reentrant activity. On the other hand, serially linked abrupt tissue expansions could form the substrate for pathways of slow conduction, which might be a part of an existing reentrant circuit. Under these circumstances, a calcium channel antagonist might terminate reentrant excitation by blocking the slow pathway. Even though peak plasma levels of nifedipine reached in humans (0.8 μM; Martens et al., 1994) are lower than those used in the present studies, the results presented suggest that L-type calcium channel antagonists might have the potential to interfere, in a complex way, with arrhythmias.

We are greatly indebted to Dr. R. Gross from Bayer for the generous gift of Bay K 8644, to R. Flückiger Labrada for production of the patterned cultures, and to Drs. A. G. Kléber and J. S. Shiner for helpful discussions on the manuscript.

REFERENCES

Bailey, J. C. 1981. Electrophysiological effects of hypertonic sucrose solutions on canine cardiac Purkinje fibers. *Circ. Res.* 49:1112–1118.

Beyer, T., J. Brachmann, and W. Kübler. 1994. Effects of dihydropyridine calcium anatagonists on intracellular action potentials of rabbit sinus node, atrium and atrioventricular node: Comparison of felodipine with nifedipine. *Drug Res.* 44:707–711.

Bukauskas, F. F., and R. Weingart. 1993. Temperature dependence of gap junction properties in neonatal rat heart cells. *Pflügers Arch.* 423: 133–139.

Cavalié, A., T. F. McDonald, D. Pelzer, and W. Trautwein. 1985. Temperature-induced transitory and steady-state changes in the calcium current of guinea pig ventricular myocytes. *Pflügers Arch.* 405: 294–296.

Cohen, N. M., and W. J. Lederer. 1987. Calcium current in isolated neonatal rat ventricular myocytes. *J. Physiol. (Lond.).* 391:169–191.

Darrow, B. J., V. G. Fast, A. G. Kléber, E. D. Beyer, and S. E. Saffitz. 1996. Functional and structural assessment of intercellular communication: increased conduction velocity and enhanced connexin expression in dibutyryl cAMP-treated cultured cardiac myocytes. *Circ. Res.* 79:174–183.

de Bakker, J. M. T., F. J. L. van Capelle, M. J. Janse, S. Tasseron, J. T. Vermeulen, N. de Jonge, and J. R. Lahpor. 1993. Slow conduction in the

infarcted human heart: 'Zigzag' course of activation. *Circulation.* 88: 915–926.

Downar, E., and M. B. Waxman. 1976. Depressed conduction and unidirectional block in purkinje fibers. *In* The Conduction System of the Heart. H. E. Stenfert Kroese B. V., Leiden. 393–409.

Fast, V. G., and A. G. Kléber. 1995a. Cardiac tissue geometry as a determinant of unidirectional conduction block: assessment of microscopic excitation spread by optical mapping in patterned cell cultures and in a computer model. *Cardiovasc. Res.* 29:697–707.

Fast, V. G., and A. G. Kléber. 1995b. Block of impulse propagation at an abrupt tissue expansion: evaluation of the critical strand diameter in 2- and 3-dimensional computer models. *Cardiovasc. Res.* 30:449–459.

Fozzard, H. A. 1990. The roles of membrane potential and inward Na+ and Ca2+ currents in determining conduction. *In* Cardiac Electrophysiology: A Textbook. Futura Publishing Company, Inc., Mount Kisco, New York. 415–425.

Goldstein, S. S., and R. Rall. 1974. Changes of action potential shape and velocity for changing core conductor geometry. *Biophys. J.* 14:731–757.

Gomez, J.-P., D. Potreau, J.-E. Branka, and G. Raymond. 1994. Developmental changes in Ca2+ currents from newborn rat cardiomyocytes in primary culture. *Pflügers Arch.* 428:241–249.

Hisatome, I., and M. Arita. 1995. Effects of catecholamines on the residual sodium channel dependent slow conduction in guinea pig ventricular muscles under normoxia and hypoxia. *Cardiovasc. Res.* 29:65–73.

Isenberg, G., and U. Klöckner. 1982. Calcium currents of isolated bovine ventricular myocytes are fast and of large amplitude. *Pflügers Arch.* 395:30–41.

Jeffrey, T., and A. Allen. 1996. Temperature dependence of macroscopic L-type calcium currents in single guinea pig ventricular myocytes. *J. Cardiovasc. Electrophys.* 7:307–321.

Jongsma, H. J., and H. E. van Rijn. 1972. Electrotonic spread of current in monolayer cultures of neonatal rat heart cell. *J. Membr. Biol.* 9:341–360.

Joyner, R. W., R. Kumar, R. Wilders, H. J. Jongsma, E. E. Verheijek, D. A. Golod, A. C. G. van Ginneken, M. B. Wagner, and W. N. Goolsby. 1996. Modulating L-type calcium current affects discontinuous cardiac action potential conduction. *Biophys. J.* 71:237–245.

Joyner, R. W., and F. J. L. Van Capelle. 1986. Propagation through electrically coupled cells: how a small SA node drives a large atrium. *Biophys. J.* 50:1157–1164.

Leon, L. J., and F. A. Roberge. 1991. Directional characteristics of action potential propagation in cardiac muscle. A model study. *Circ. Res.* 69:378–395.

Luo, C.-H., and Y. Rudy. 1994. A dynamic model of the cardiac ventricular action potential. I. Simulations of ionic currents and concentration changes. *Circ. Res.* 74:1071–1096.

Martens, J., P. Banditt, and F. P. Meyer. 1994. Determination of nifedipine in human serum by gas chromatography-mass spectrometry: validation of the method and its use in bioavailability studies. *J Chromatogr. B.* 660:297–302.

Matsuda, K., A. Kamiyama, and T. Hoshi. 1967. Configuration of the transmembrane potential of the Purkinje-ventricular fiber junction and its analysis. *In* Electrophysiology and Ultrastructure of the Heart. Grune & Stratton, Inc., New York. 177–178.

Mendez, C., W. J. Mueller, and X. Urguiaga. 1970. Propagation of impulses across the Purkinje fiber-muscle junction in the dog heart. *Circ. Res.* 26:135–150.

Mitchell, M. R., T. Powell, D. A. Terrar, and V. W. Twist. 1983. Characteristics of the second inward current in cells isolated from rat ventricular muscle. *Proc. R. Soc. Lond. B.* 219:447–469.

Osaka, T., B. M. Ramza, R. C. Tan, and R. W. Joyner. 1989. Developmental changes in the electrophysiologic properties of rabbit papillary muscles. *Pediatr. Res.* 26:543–547.

Overholt, E. D., R. W. Joyner, R. D. Veenstra, D. Rawling, and R. Wiedmann. 1984. Unidirectional block between Purkinje and ventricular layers of papillary muscle. *Am. J. Physiol.* 247:H584–H595.

Ozaki, S., H. Nakaya, Y. Gotoh, M. Azuma, O. Kemmotsu, and M. Kanno. 1989. Effects of halothane and enflurane on conduction velocity and maximum rate of rise of action potential upstroke in guinea pig papillary muscles. *Anesth. Analg.* 68:219–225.

Robinson, R. B. 1982. Action potential characteristics of rat cardiac cells do not change with time in culture. *J. Mol. Cell Cardiol.* 14:367–370.

Rohr, S. 1986. Temperature-controlled perfusion chamber suited for mounting on microscope stages. *J. Physiol. (Lond.).* 378:90.

Rohr, S., A. G. Kléber, and J. P. Kucera. 1996. Induction of very slow and discontinuous conduction by palmitoleic acid in linear strands of rat ventricular myocytes. *Biophys. J.* 70:278*a*. (Abstr.).

Rohr, S., and J. P. Kucera. 1995. The calcium inward current can play a critical role for the success of impulse propagation across expansions of cardiac tissue in the presence of the sodium inward current. *Circ. Res.* 92:2064,I-432.

Rohr, S., and B. M. Salzberg. 1994a. Characterization of impulse propagation at the microscopic level across geometrically defined expansions of excitable tissue: multiple site optical recording of transmembrane voltage (MSORTV) in patterned growth heart cell cultures. *J. Gen. Physiol.* 104:287–309.

Rohr, S., and B. M. Salzberg. 1994b. Multiple site optical recording of transmembrane voltage in patterned growth heart cell cultures: assessing electrical behavior, with microsecond resolution, on a cellular and subcellular scale. *Biophys. J.* 67:1301–1315.

Rohr, S., D. M. Schölly, and A. G. Kleber. 1991. Patterned growth of neonatal rat heart cells in culture. Morphological and electrophysiological characterization. *Circ. Res.* 68:114–130.

Simpson, P. 1985. Stimulation of hypertrophy of cultured neonatal rat heart cells through an α1-adrenergic receptor and induction of beating through an α1- and β1-adrenergic receptor interaction. *Circ. Res.* 56:884–894.

Streit, J., and H. D. Lux. 1989. Distribution of calcium currents in sprouting PC12 cells. *J. Neurosci.* 9:4190–4199.

Sugiura, H., and R. W. Joyner. 1992. Action potential conduction between guinea pig ventricular cells can be modulated by calcium current. *Am. J. Physiol.* 263:H1591–H1604.

Ursell, P. C., P. I. Gardner, A. Albala, J. J. Fenoglio, and A. L. Wit. 1985. Structural end electrophysiological changes in the epicardial border zone of canine myocardial infarcts during infarct healing. *Circ. Res.* 56: 436–451.

Veenstra, R. D., R. W. Joyner, and D. A. Rawling. 1984. Purkinje and ventricular activation sequences of canine papillary muscle. Effects of quinidine and calcium on the purkinje-ventricular conduction delay. *Circ. Res.* 54:500–515.

Yatani, A., and A. M. Brown. 1985. The calcium channel blocker nitrendipine blocks sodium channels in neonatal rat cardiac myocytes. *Circ. Res.* 57:868–875.

Yatani, A., D. L. Kunze, and A. M. Brown. 1988. Effects of dihydropyridine calcium channel modulators on cardiac sodium channels. *Am. J. Physiol.* 254:H140–H147.